Scalable Synthesis of Noble Metal Nanoparticles

Venugopal Santhanam

Abstract Noble metal nanoparticles possess unique size-dependent electronic and optical characteristics and are one of the foremost 'building blocks' for nanostructured device fabrication. As such, there is considerable interest in developing continuous-flow processes for large-scale synthesis of noble metal nanoparticles. In this chapter, we describe the results of our work aimed at understanding key process variables that determine particle size distribution in two popular protocols used for lab-scale synthesis of gold and silver colloids. Our understanding of the importance of aggregation and role of the pH of precursor solutions in determining the kinetics and stability of colloidal sols enabled us to propose suitable modifications in process conditions that enabled scalable synthesis of gold and silver nanoparticles. These insights also led to the development of a novel route for low-cost fabrication of silver nanostructures on paper using an inkjet printer.

Keywords Metal nanoparticles • Continuous synthesis • Effect of pH • Mode of addition • Reactive inkjet printing

1 Introduction

The expectation of an impending nanotechnology revolution, which promises faster, cheaper and portable solutions for energy, healthcare and environmental issues, has captured the imagination of laymen. The nanoscale regime (ca. 1–100 nm) corresponds to an intermediate size range, between a molecular state and the bulk state; it encompasses several characteristic length scales over which collective properties emerge. For example, answers to questions on transition from atomic to bulk behaviour, such as 'what is the size at which the electron energy levels in a collection of atoms lose their discrete nature and become delocalised over the entire structure?', have been found to lie in this size range. Such information is of considerable interest to scientists for understanding behaviour of condensed state

V. Santhanam (✉)
Department of Chemical Engineering, Indian Institute of Science, Bangalore 560012, India
e-mail: venu@chemeng.iisc.ernet.in

© Springer India 2015

Y.M. Joshi, S. Khandekar (eds.), *Nanoscale and Microscale Phenomena*,
Springer Tracts in Mechanical Engineering, DOI 10.1007/978-81-322-2289-7_4

joshi@iitk.ac.in

matter. The tantalising possibility of harnessing such knowledge for controlling material properties in a 'digital/discrete' manner, by varying system size, is one of the leading reasons for the buzz surrounding the term 'nanotechnology'. Nanomaterials, objects with one or more dimensions in the nanoscale regime, are expected to play a critical role as 'building blocks' in the field of nanotechnology. Metal or semiconductor or carbon-based nanostructures with different morphologies, e.g. nanoparticles, nanowires/nanotubes, nanoscale films, have been widely studied. Noble metal nanoparticles are the foremost contenders amongst nanomaterials that already have a significant market presence [1], a presence that is more likely to expand as several technologies such as drug delivery [2], nanoelectronics [3], etc. mature in the near future.

The use of noble metal nanoparticles in itself is not unique to the recent past, historical examples of their uses abound. For example, noble metal nanoparticles were used to fabricate stained glass windows in Europe, and colloids of noble metal nanoparticles were part of traditional medicines/biocides in India [4]. More recently, the use of gold nanoparticles as contrast agents for electron microscopy and point-of-care biomedical test kits are examples of nanoparticle-based commercial applications [5]. What sets apart the current research and development studies from previous efforts is the ability to characterise and manipulate the nanomaterials at the atomic scale and the resulting improved understanding of the science behind their distinctive properties.

From a process engineering perspective, the importance of research on scalable processes for producing metal nanoparticles with controlled sizes is evident. To pursue such questions, a laboratory for nanoparticle engineering was established at IISc, Bangalore, under the IRHPA scheme of DST, and this chapter summarises our research on scalable synthesis of metal nanoparticles, especially gold and silver nanoparticles. In the following, an introduction to some novel properties of noble metal nanoparticles is presented, followed by a perspective on the questions posed as we began our research on scaleup of colloidal nanoparticle synthesis. Then, the results of our investigations on the synthesis of gold and silver nanoparticles using either tannic acid or sodium citrate as both reducing and stabilising agents are presented. Finally, a summary of the key research findings is presented.

2 Properties of Noble Metal Nanoparticles

A striking attribute of colloidal dispersions of noble metal nanoparticles is their colour. Noble metal nanoparticles exhibit strong plasmon resonance absorbance bands in the visible spectrum that are size and shape dependent, resulting in the ability to tune colour without changing the material used. The surface plasmon resonance bands result from the interaction of incident electromagnetic field ('light') with the metal nanoparticles leading to coherent oscillations of the conduction band electrons. The coherently oscillating electrons behave as an entity denoted as plasmons.

joshi@iitk.ac.in

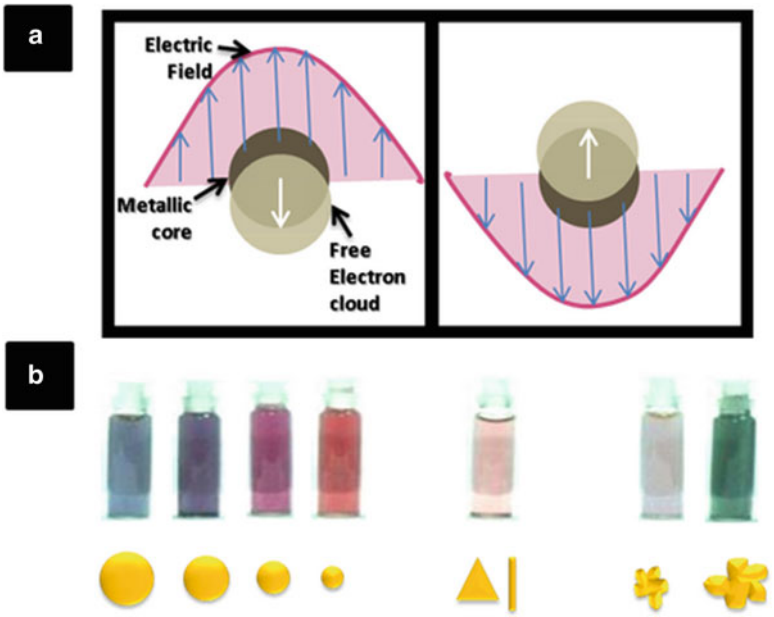

Fig. 1 (**a**) Schematic diagram representing the interaction of light with metal nanoparticles (figure not to scale). The interaction of electromagnetic field with the metal nanoparticles results in coherent oscillations of the conduction band electrons. The *circles* are a guide to illustrate the collective displacement of the mobile electrons (plasmons) within the nanoparticles from the ionic cores. The two panels illustrate the movement of electrons corresponding to two different phases of the incident radiation's electric field. (**b**) Distinct colours exhibited by aqueous sols of gold nanoparticles synthesised during the course of our research. The cartoons, underneath the sols, depict the morphology of nanostructures present in the respective sols (Color figure online)

Figure 1a shows a schematic representation of the interaction of electromagnetic light waves with metal nanoparticles that are much smaller than the wavelength of the incident light. The conduction band electrons within the nanoparticle interact with the time-varying electric field of the incident light and lead to the formation of an oscillating dipole (in the simplest case). A large enhancement in the light absorption results when the wavelength of the incident light matches the size-dependent resonant frequency of the dipole (plasmon resonance). As the restoring force is proportional to the surface area in such systems and also confined by the nanoparticle, these are commonly referred to as localised surface plasmon resonances (LSPR). Figure 1b showcases the range of colours exhibited by aqueous sols of gold nanoparticles having different sizes and shapes that were synthesised during the course of this work.

The electronic properties of small metal particles have also been investigated extensively. The simplest system studied consists of placing a single metal nanoparticle between two electrodes with tunnelling barriers separating the electrodes from the metal nanoparticle [6]. In this configuration (Fig. 2), the electrical conduction

joshi@iitk.ac.in

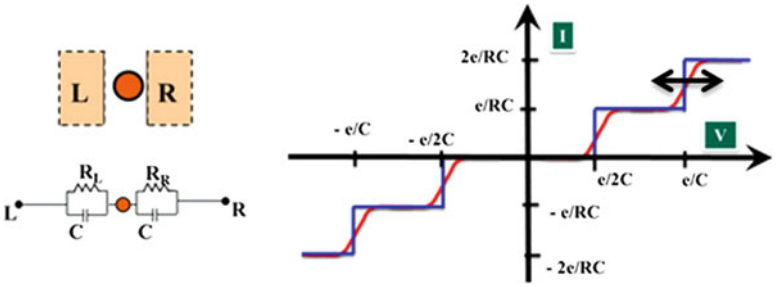

Fig. 2 Schematic representation and equivalent circuit of nanostructure consisting of a metal nanoparticle placed between two electrodes, and Ideal I-V curves (*double headed arrow* indicates the smearing of coulomb staircase at temperatures >0 K) for this nanostructure illustrating the phenomena of Coulomb blockade and Coulomb staircase

is entirely suppressed at low bias voltages. This phenomenon is called 'Coulomb blockade'. Coulomb blockade occurs when the electrostatic energy increase due to the addition of a single electron onto a capacitatively coupled metal island is much larger than the thermal energy of the electrons:

$$e^2/2C >> k_B T \tag{1}$$

where 'e' is the charge on an electron, 'C' is the effective capacitance of the metal island, 'k_B' is the Boltzmann constant and 'T' is the absolute temperature of the metal island. In the case of metal nanoparticles, the capacitance, 'C', is directly proportional to the radius of the metal nanoparticle. At room temperature, metal particles with radius less than 2–3 nm satisfy Eq. 1. Furthermore, for Coulomb blockade to be observed, the tunnelling resistance (R) to and from the metal island must also be much greater than the resistance quantum (R_Q):

$$R >> R_Q \tag{2}$$

where $R_Q = h/2e^2$ ($\sim$12.9 kΩ) with 'h' being the Planck constant.

Bulk metals typically exhibit a linear I-V response, which is characterised by the well-known Ohm's law. In contrast, when both Eqs. 1 and 2 are satisfied, the I-V curve for an asymmetric tunnelling junction [$R_R >> R_L$ or $R_L >> R_R$] shows characteristic steps in current, denoted as 'Coulomb staircase' (Fig. 2). Due to asymmetry in electron transport rates between the two junctions, electrons tend to accumulate on the isolated metal nanoparticle; the electrostatic energy associated with such charging of the 'island' has to be compensated for by increasing the external bias. This leads to a nonlinear I-V response. Such sequential tunnelling phenomena can give rise to the ability to control the charge on the island at single electron level and form the basis of the field of single electronics.

joshi@iitk.ac.in

3 Synthesis of Noble Metal Nanoparticles: Prevalent Status and Identified Research Needs

Historically, the synthesis of metal nanoparticles predates modern science. The Lycurgus chalice of Rome, belonging to the fifth century, contains gold and silver nanoparticles; Mayan blue pigment from the eleventh century contains iron and chromium nanoparticles [7]; Swarna Bhasma, an Ayurvedic medicine dating back to 2000 BC, contains gold nanoparticles [4]. The report by Faraday, in 1857, on the preparation of a gold colloidal solution by reacting chloroauric acid with white phosphorus has come to be regarded as the beginning of scientific studies into the synthesis of noble metal nanoparticles [8]. Faraday postulated that the red colour of both aqueous gold solutions as well as the ruby colour of stained glasses found in medieval churches was due to the presence of very fine gold particles. At the beginning of the twentieth century, the development of the ultramicroscope led to the finding that such colloidal solutions contained 'millimicron' size particles [9]. From 1950s onwards, metal nanoparticles have been utilised as contrast-enhancing agents for the imaging of cells [10] using electron microscopes, which spurred extensive investigations into the different recipes available for the synthesis of nanoparticles.

Presently, synthesis procedures used for generating metal nanoparticles can be classified into two broad classes – (1) extruding/grinding/sculpting bulk materials (top-down approach) and (2) initiating nucleation and growth of desired atomic/reactive precursors (bottom-up approach). The top-down approaches are easily amenable to continuous-flow processing but suffer from the following disadvantages: they are energy intensive, they produce particles with a very broad size distribution, they are limited in their capability to produce particles with diameters in the range of 1–20 nm, and they can also introduce contamination due to the tools involved. Bottom-up approaches involving liquid-phase recipes are more widely prevalent in research laboratories and are routinely used for batch synthesis. To control the size of nanoparticles, parameters such as molar ratio of reducing agent to metal salt (MR) [10–12], molar ratio of capping agent to metal salt [13], and temperature [12] have been varied. Liquid-phase synthesis has typically been portrayed as simple 'recipe' for carrying out redox reactions at the lab scale, but the complexity of underlying nucleation and growth processes poses formidable challenges for scaling such recipe into continuous-flow processes.

Metal nanoparticles, especially gold and silver nanoparticles in the size range of 2–20 nm, are well suited for applications in nanoelectronics. A focus of our project was the development of scalable processes for synthesis of monodisperse metal nanoparticles for such applications. Desired characteristics were that the process should be easily scalable, and occur at room temperature, to simplify reactor design considerations. Recently, there is an increasing emphasis on using greener routes. 'Green chemistry' is defined as the design of chemical products and processes that reduce or eliminate the use and generation of hazardous substances [14]. In this context, synthesis of nanoparticles in the aqueous phase using environmentally

joshi@iitk.ac.in

benign reagent is more desirable for large-scale synthesis. Sodium citrate (used in 'citrate method') and a combination of sodium citrate and tannic acid (used in 'Slot and Geuze method') are the two most commonly used 'green' reagents, as these reagents can act as both reducing and stabilising agents for the synthesis of metal nanoparticles. The reported size range of particles synthesised at elevated temperatures, using these reagents, varies from 10 to 100 nm. For the rapid, room temperature synthesis of metal nanoparticles, hazardous reducing agents like sodium borohydride and hydrazine [15] were used. A common refrain for the use of such hazardous reagents was their 'strength', usually inferred from the difference in standard redox potential values between the reducing agent and bulk metal.

Interestingly, we observed that the reduction of chloroauric acid by citrate is faster when some tannic acid was added to the citrate, although both citrate and tannic acid have comparable redox potentials. This observation challenged the prevalent notions of metal nanoparticle synthesis by redox reactions in solutions. To understand the reasons behind these observations, we carried out systematic studies to elucidate the factors controlling the kinetics of nanoparticle formation using the two most widely used reagents for the synthesis of gold and silver nanoparticles, namely, citrate and tannic acid. The results of our investigations are presented and discussed in the following sections.

4 Room Temperature 'Green' Synthesis of Noble Metal Nanoparticles

4.1 Tannic Acid as Reducing Agent

Tannic acid, also known as tannin, is a polyphenolic compound derived from plants like gall nuts, tree barks, etc. Ostwald, in 1912, utilised tannin to reduce chloroauric acid at 100 °C and stabilise gold nanoparticles [16]. Ostwald reported that tannin can reduce chloroauric acid at neutral pH to form stable gold nanoparticles at 100 °C, even if tap water is used to prepare the aqueous solutions. Turkevich [12] replicated Ostwald's protocol and reported the particle size to be 12.0 ± 3.6 nm based on TEM images. Mulphrodt [17] used tannic acid along with citrate to reduce the size of nanoparticles synthesised to values lower than that obtained by citrate method. Slot and Geuze [10] further modified the protocol and controlled the size of nanoparticles from 3.5 to 15 nm by varying the concentration of tannic acid in the synthesis, while the concentration of citrate remained constant. Tannin has also been used to synthesise silver nanoparticles at 60 °C [18]. Aqueous solution of tannic acid is found to be weak reducing agent, at room temperature, which can only grow seeds into nanoparticles [19]. Hence, higher temperatures were used for the nucleation and growth of silver and gold nanoparticles using tannic acid. Thus, although tannic

joshi@iitk.ac.in

acid has been known to reduce and stabilise metal nanoparticles, neither were the reported procedures performed at room temperature nor were monodisperse nanoparticles obtained in the size range of 1–10 nm.

4.2 *Factors Affecting Kinetics of Silver Nanoparticle Formation [20]*

The pKa of tannic acid solution falls between seven and eight, depending on the extent of dissociation of tannic acid [21], which is known to partially hydrolyse under mild acidic/basic conditions into glucose and gallic acid units [22]. Gallic acid at alkaline pH reduces silver nitrate into silver nanoparticles rapidly at room temperature [23], but the particles form aggregates in solution as gallic acid is a poor stabilising agent. Glucose is a weak reducing agent at room temperature, but it is an excellent stabilising agent at alkaline pH [24]. These findings suggested to us that tannic acid could be an ideal reducing and stabilising agent under alkaline conditions at room temperature.

A few experiments were performed to understand the role of pH of tannic acid in the synthesis of metal nanoparticles. Five millilitre of 2.95 mM solution of $AgNO_3$ was added to 20 mL of tannic acid solution, maintained at the desired pH. Figure 3 shows the hydrodynamic diameter of silver nanoparticles synthesised by varying the initial pH of tannic acid used in the reaction. At acidic pH values, nanoparticle formation was not observed even after waiting for several hours. From a pH value of 6 onwards, nanoparticle formation was observed to occur in a matter of minutes, with both size and time for appearance of colour (due to SPR band of silver colloids) decreasing rapidly till a pH of 8. Further increase in the pH did not cause a significant decrease in the hydrodynamic size.

To understand the kinetics, the stoichiometric ratio required for the completion of the reaction between tannic acid and silver nitrate was investigated. Figure 4 shows UV-Vis spectra of 0.25 mL aliquots sampled during the stepwise addition

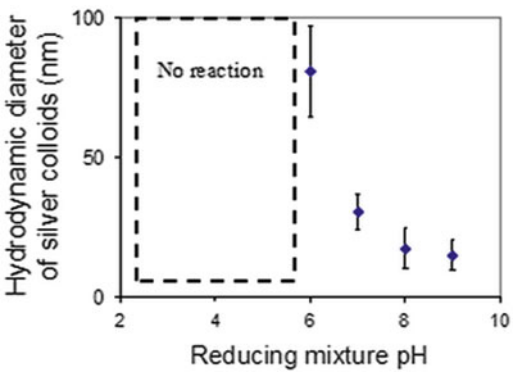

Fig. 3 Effect of pH at room temperature. Variation of hydrodynamic diameter of silver nanoparticles as a function of initial pH of tannic acid solution. There is no noticeable reaction for pH values <6. [$AgNO_3$] = 0.59 mM, MR = 0.05

joshi@iitk.ac.in

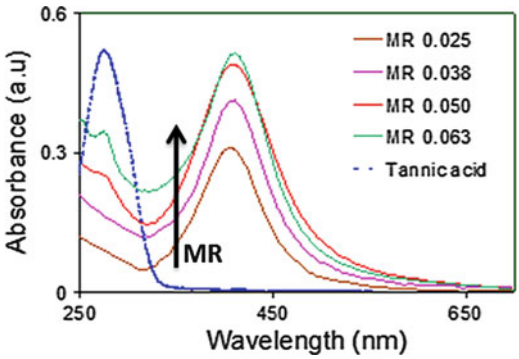

Fig. 4 UV visible spectra of silver nanoparticle solutions as a function of the molar ratio of tannic acid to silver nitrate (MR). The spectrum of a concentrated (2× original) tannic acid solution is also shown for comparison (Reproduced with permission from [24])

(corresponding MR values provided in the legend) of tannic acid solution, maintained at a pH of 8, to 5 mL of 2.95 mM silver nitrate solution. It is seen that the surface plasmon peak of silver nanoparticles at 420 nm increases initially and then saturates at an MR value of 0.05, indicating that silver nitrate is completely reduced. Also, for MR values $\geq$0.05, a small shoulder at 270 nm is seen and is attributed to the presence of excess tannic acid. The spectrum of a concentrated solution of pure tannic acid at pH 8 is also shown for comparison. A stoichiometric ratio of tannic acid to silver nitrate of 0.05 indicates that one mole of tannic acid can reduce 20 moles of silver nitrate.

Figure 5a shows the variation in hydrodynamic size of silver nanoparticles with the molar ratio of tannic acid to silver nitrate; the MR was varied by increasing the tannic acid concentration at a constant value of the silver nitrate solution. An increase in the MR value increases the hydrodynamic diameter of silver nanoparticles. To analyse the role of excess tannic acid, the nanoparticle synthesis was monitored by studying the evolution of absorbance at SPR peak wavelength with millisecond resolution in stop-flow module (Fig. 5b). From Mie theory, the absorbance is directly proportional to the volume of nanoparticles (for size <20 nm). The induction time, which is inversely proportional to the nucleation rate, increases with increasing MR. Also, the initial slope of the absorbance profile is higher for smaller MR indicating that the growth rate is higher at smaller MR. Figure 5c–e shows representative Field Emission Scanning Electron Microscope (FESEM) and TEM images for these samples. The trends of lower nucleation and growth rates, corresponding to increasing particle size, with increasing MR are counterintuitive. Intuitively, one expects that increasing reducing agent concentration should increase redox reaction rates and, therefore, result in higher growth and nucleation rates. Also, the observed trends cannot be interpreted in terms of the role of tannic acid as a stabiliser, as increasing stabiliser concentration is also expected to result in smaller sizes. This implies that the role of tannic acid is not limited to that of reducing/stabilising agent.

joshi@iitk.ac.in

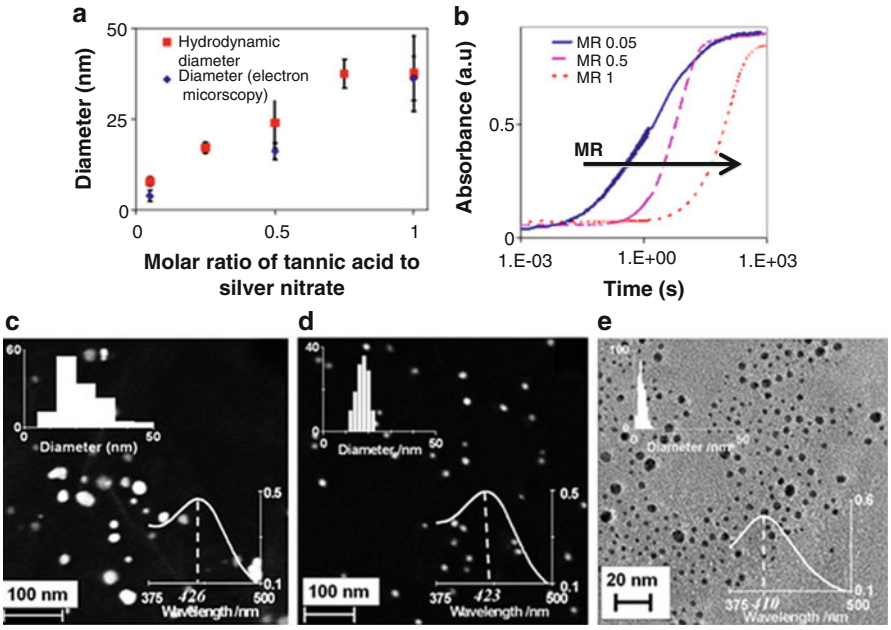

Fig. 5 (**a**) Change in the hydrodynamic diameter of silver nanoparticles with the molar ratio of tannic acid to silver nitrate. (**b**) Time evolution of absorbance at SPR peak wavelength for different initial molar ratios of tannic acid to silver nitrate (MR). The absorbance rises faster for lower MR values. Representative electron microscopy images of silver nanoparticles synthesized at various MR values. (**c**) MR = 1 (FESEM), (**d**) MR = 0.5 (FESEM), (**e**) MR = 0.05 (TEM). The inset graphs in (**c**–**e**) depict the corresponding particle size distribution and UV–Vis spectrum, with ordinates representing the actual number of particles counted and absorbance (a.u.) respectively (Reproduced with permission from [24])

4.3 Tannic Acid as Organiser

A representative structure of tannic acid, corresponding to its average formula weight, is shown in Fig. 6. It consists of a central core of glucose that is linked by ester bonds to polygalloyl ester chains. Tannic acid has 25 phenolic hydroxyl (−OH) groups in its structure, but only ten pairs of 'ortho'-dihydroxyphenyl groups are capable of taking part in redox reactions to form quinones and donate electrons, because of the chelating action of adjacent hydroxyl groups and constraints on carbon valency. Hence, each tannic acid molecule is capable of donating 20 electrons; this value matches well with the number deduced experimentally. At alkaline pH, the deprotonation of phenolic hydroxyl groups will enhance their chelation with cations and can thus account for their enhanced reactivity. But the ability to nucleate nanoparticles cannot be explained by this fact alone, as their redox potentials are still lower than that required to completely reduce isolated metal ions in solution. This suggests a third role for tannic acid as an 'organiser' of ions/atoms

joshi@iitk.ac.in

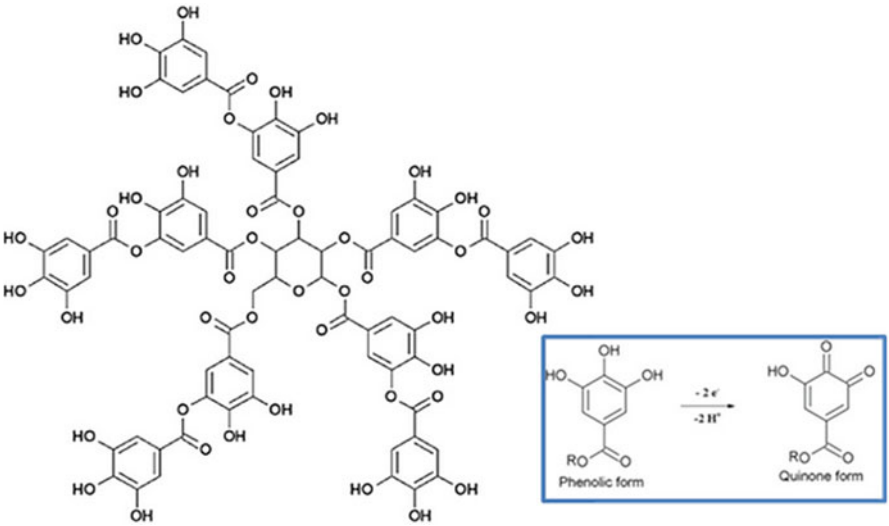

Fig. 6 Representative structure of tannic acid ($C_{76}H_{52}O_{46}$). The *inset* on the right shows the phenol to quinone conversion upon oxidation of tannic acid

for facilitating nucleation, given that a single tannic acid molecule can chelate with multiple ions and reduce them. Such a mechanism is consistent with the fact that the redox potential value for metal clusters varies rapidly with increasing cluster size, from values corresponding to a strong reducing agent for a single atom (i.e. thermodynamically unfavourable conditions for reduction by tannic acid) to that of an oxidant (similar to the bulk, and reducible by tannic acid) for clusters having a few tens of atoms [25], thereby enabling 'weak' reducing agents to nucleate metal nanoparticles. The mechanism by which reduction and atomic reorganisation occur within such chelation complexes is a matter for further investigation.

The role of 'organiser' is also consistent with the observed trends of nucleation and growth rates of silver nanoparticles as a function of MR. Tannic acid has five units of gallic acid and each gallic acid unit can combine with four silver ions. Each tannic acid molecule can be thought of as a five-armed chelator. Thus, at an MR of 0.05, tannic acid complexes will be saturated with 20 silver atoms enabling rapid nucleation (faster induction time) that results in smaller particle size. At MR of 1, each tannic acid is on average ligated to only one silver atom and so the nucleation rate will be decided by the interaction of such 'unsaturated' compounds in solution leading to slower nucleation rate (larger induction times) that results in larger particle sizes. The reduction in the initial growth rate with an increasing MR can also be accounted for by considering that growth occurs due to collision of nuclei/particles with chelated silver atoms. On an average, rate of collision between chelated silver atoms and nuclei/particle will be similar in all cases due to opposing effects of increasing concentration and decreasing ligation; however, the probability of incorporation per collision will be higher for compounds ligated with a higher

joshi@iitk.ac.in

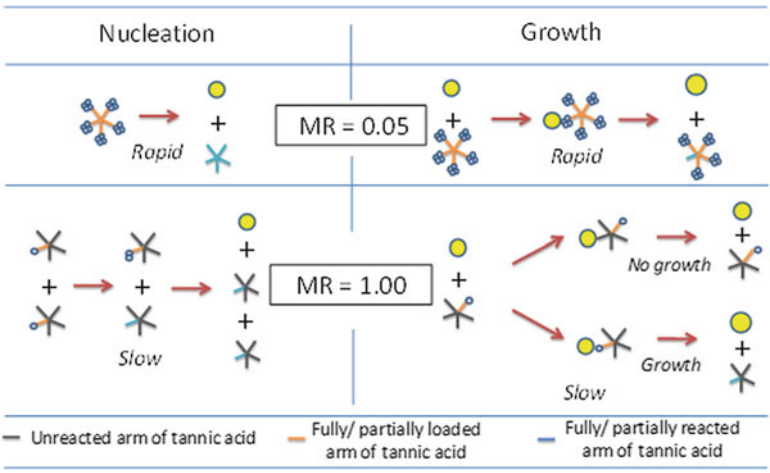

Fig. 7 Schematic representation of organiser-based nucleation and growth processes at MR values of 0.05 and 1. Tannic acid is represented as a five-armed molecule with each arm capable of reducing and chelating with four silver atoms. Both nucleation and growth processes are faster at MR value of 0.05 as compared to MR value of 1 resulting in the rapid formation of smaller nanoparticles at the lower MR value. Note: the number of loaded atoms depicted is representative of the mean value, given that all the silver ions are reduced and chelated (Color figure online) (Reproduced with permission from [20])

number of silver atoms. Thus, at smaller MR values, the incorporation efficiency of atoms onto nuclei/particles (i.e. growth) will be higher per collision resulting in higher growth rates. Figure 7 illustrates these concepts at MR values of 0.05 and 1.

4.4 Interplay Between Reactivity and Stabilisation in the Synthesis of Gold Nanoparticles [26]

Chloroauric acid, the most common gold precursor used, possesses pH-dependent reactivity. At acidic pH, gold ion complexes with chloride ligands are predominant, while at basic pH, gold ions complexed with hydroxyl ligands are predominant. The chloride ligand can be easily displaced as compared to the hydroxyl ligand, resulting in higher reactivity of chloroauric acid at acidic pH values. On the other hand, nucleation and growth of nanoparticles by tannic acid occur rapidly at alkaline pH. Faced with these conflicting requirements and to identify optimal conditions for rapid, room temperature synthesis of gold nanoparticles, a series of experiments were carried out by varying the initial pH of the two reagents (prior to mixing). Three millilitre of 4.4 mM tannic acid solution at desired pH was added to 22 mL of 0.288 mM chloroauric acid solution at desired pH. The resulting colloidal samples were characterised using TEM to determine particle size, using a stop-flow reactor (SFR) to determine induction time, and ζ-potential measurements. These results are summarised in Table 1.

joshi@iitk.ac.in

Table 1 Experimental conditions and characterisation results for synthesis of gold nanoparticles

Experiment	Initial pH of chloroauric acid solution	Initial pH of tannic acid solution	pH of reaction mixture	Particle diameter ($\mu \pm \sigma$), nm	Induction time, *s*	ζ-potential, mV
A	3.2	3.1	3.2	14.1 ± 4.8	3	-20 ± 2
B	3.2	7.1	6.4	7.1 ± 1.6	1.5	-49 ± 2
C	7.0	6.3	6.4	10.7 ± 3.8	66.8	-69 ± 2
D	9.1	3.1	6.4	14.2 ± 5.4	163.5	-60 ± 2
E	2.1	7.1	5.0	10.0 ± 2.9	0.9	-18 ± 7
F	2.1	9.0	7.1	5.8 ± 1.0	0.5	-35 ± 7

Comparison of the results of these experiments in terms of the kinetics (induction time), stability (ζ-potential) and particle size shows the following: (1) the initial pH of chloroauric acid solution mainly controls the kinetics (A-D; B-C), whereas the pH of tannic acid has only a slight influence on kinetics (A-B; E-F). The fact that initial pH of the reagents, prior to mixing, has a significant impact implies that the kinetics of forming less reactive hydroxy-chloroauric species, after a step change in pH from acidic to neutral conditions, is slower than that of the redox reaction; (2) the pH of the reaction mixture determines the stability, and the final particle size is more sensitive to variations in stability (B-E; A-D) rather than kinetics (B-C-D;C-E). This suggests that aggregation is an important pathway in the formation of the nanoparticles and that it is minimised at reaction mixture pH values of 6.4 and above. All the colloidal sols were stable upon storage for more than a year, indicating that aggregation is active only during the early growth stages.

Overall, these results show that gold nanoparticle size distribution is determined by a fine balance between the reactivity of precursors and coalescence in the initial period, which can be manipulated by controlling the initial pH of reactants and the reaction mixture pH, respectively. Figure 8 illustrates the various pathways involved. A key outcome is that independent control over reactivity and stabilisation can be achieved by manipulating the pH of the precursor solutions. The detailed investigation of the role of molar ratio and the pH of tannic acid showed that it is plausible to synthesise nanoparticles with various morphologies at room temperature. Surprisingly, the polydispersity of nanoparticles synthesised under various conditions remained high (>15 %).

Given that alkaline pH is more favourable for preventing aggregation, an experiment ('G') was carried out to minimise coalescence during mixing by altering the order of addition. This was achieved by simply reversing the order of addition (i.e. chloroauric acid into tannic acid) while maintaining the initial pH of reagents, overall amount of reagents, the volume of the added reagent and the volume of the total reaction mixture at values used in experiment 'B'. For comparison, a 1 mL sample was prepared by rapidly mixing (∼ within 3 ms) the two reagents in stop-flow module (experiment H), while maintaining the concentration, initial pH and volumetric ratio similar to experiment 'B'. The corresponding size distributions

joshi@iitk.ac.in

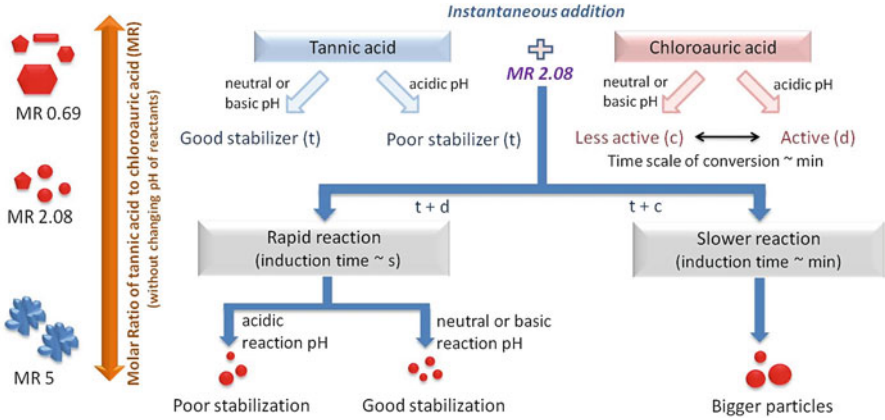

Fig. 8 Schematic summary of the effect of MR and the roles of reagent and the reaction mixture pH in determining gold nanoparticle size and shape (Color figure online) (Reprinted from [26] under CCA terms)

were determined to be 5.9 ± 1.6 nm (G) and 6.2 ± 1.9 nm (H), respectively. The effect of mode as well as speed of mixing on size distribution is minimal indicating that stabilisation of nanoparticles by adsorption of tannin requires a finite time during which particles may coalesce.

Attempts to minimise coalescence by using an excess of tannic acid did not yield the desired result. So, the next best strategy was to add diluted chloroauric acid slowly into tannic acid to provide adequate time for adsorption of tannin. Experiment 'I' was conducted by adding chloroauric acid at a rate of ~1 mL/min into tannic acid, while maintaining overall concentration and total volume of the reaction mixture constant as in experiment 'G'. Representative TEM images and corresponding particle size distributions of aliquots collected during different stages of addition are shown in Fig. 9. These results clearly show that the slow addition of chloroauric acid into tannic acid is the best strategy to synthesise monodisperse gold nanoparticles. This process can be easily extended to form size-controlled nanoparticles with larger mean size, if care is taken to ensure that the reaction mixture pH never falls below 6.4.

The constant value of standard deviation estimates (0.6–0.8 nm) indicates that the growth mode is polynuclear surface reaction controlled (i.e. the growth rate is independent of particle size). Mass balance requirement for surface reaction-controlled growth dictates that increase in mean nanoparticle diameter must be proportional to 1/3 power of the volume of chloroauric acid added. Figure 10 shows a plot of the predicted and the observed mean diameters as a function of the 1/3 power of the volume of chloroauric acid added. The observed values are seen to agree exceptionally well with the predicted values, which is a clear indication that the slow (dropwise) addition protocol is akin to one-shot process for seed formation followed by their controlled growth into nanoparticles.

joshi@iitk.ac.in

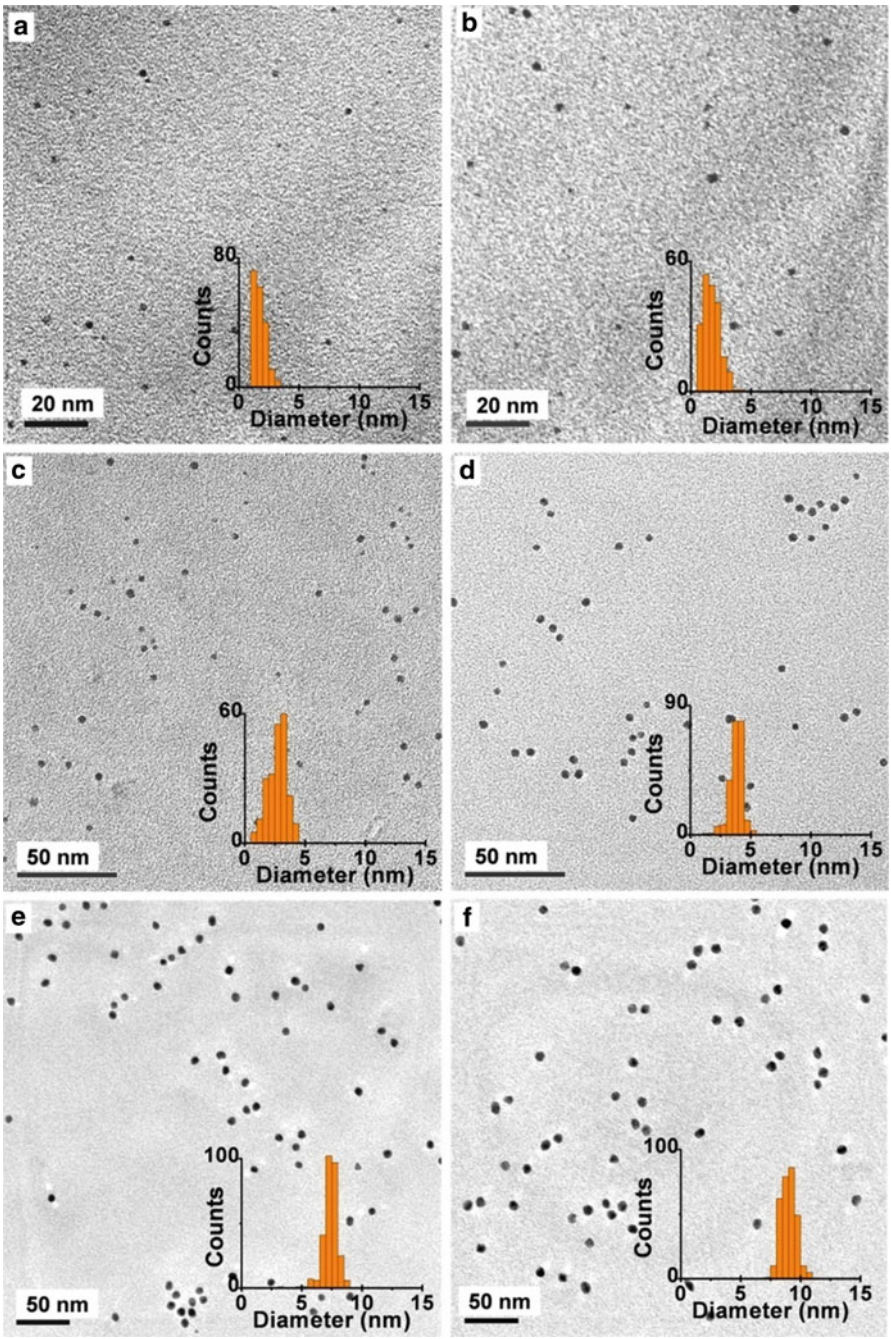

joshi@iitk.ac.in

4.5 *Monodisperse Sub-10 nm Gold Nanoparticles by Reversing the Order of Addition in Citrate Method [27]*

The 'classical citrate' method for synthesising gold nanoparticles, using sodium citrate as the reducing agent, is renowned for its ability to produce biocompatible colloids with a mean size >10 nm. Biocompatibility and ease of surface functionalisation have made the citrate method not only popular amongst researchers but also the method of choice for producing NIST reference standards for biological applications (NIST Reference Materials 8011, 8012 and 8013). Citrate-stabilised gold nanoparticles in the 1–10 nm size range are desirable for their ability to target the cell nucleus for gene/drug delivery and for the significant nanoscale size effects that occur in this size range.

Turkevich [12] showed that dicarboxy acetone, formed due to oxidation of citrate by chloroauric acid, facilitates nucleation of gold nanoparticles. Kumar et al. [28] have modelled the formation of gold nanoparticles by the citrate reduction method and elucidated the role of dicarboxy acetone as an 'organiser' for nucleation. Also, citrate exhibits pH-dependent ionisation and is an effective stabilising agent at alkaline pH. Based on our insights into the formation of gold nanoparticles by reduction with tannic acid, we hypothesised that smaller nanoparticles can be formed by reversing the order of addition, i.e. adding reactive chloroauric acid at acidic pH into alkaline solution of sodium citrate. 0.25 mL of 25.4 mM of chloroauric acid (measured pH of 1.6) was added to 24.75 mL of boiling citrate solution of required concentration. For comparison, we also carried out experiments wherein the same total amount (moles) of reagents was added in the standard configuration, i.e. adding 0.25 mL of sodium citrate solution of the desired concentration into 24.75 mL of boiling 0.256 mM chloroauric acid solution. Figure 11 shows some representative images and also compares the sizes of gold nanoparticles formed by these two alternative modes of addition.

At MR >5, addition of chloroauric acid into citrate solution, indeed, results in smaller nanoparticles than adding the alternative way. Figure 12a–b shows the digital images of the reaction mixture during the synthesis. The time required for the synthesis of nanoparticles was also found to be faster while adding chloroauric acid into citrate solution. Unlike classical citrate reduction, where citrate solution at room temperature is added to the reaction mixture, here, boiling citrate solution

Fig. 9 Representative TEM image of size-controlled nanoparticles formed by slow (dropwise) addition protocol. *Insets* show size distribution histograms. Nanoparticles were synthesised by slow (∼1 mL/min) addition of (**a**) 0.2 mL, (**b**) 0.4 mL, (**c**) 2 mL, (**d**) 5 mL and (**e**) 40 mL of 0.64 mM chloroauric acid into 15 mL of 0.89 mM tannic acid, while maintaining reaction mixture pH above 6.4. The nanoparticle size distributions are (**a**) 1.7 ± 0.5 nm, (**b**) 1.8 ± 0.7, (**c**) 2.7 ± 0.8 nm, (**d**) 3.8 ± 0.6 nm and (**e**) 7.4 ± 0.6 nm. In (**f**), nanoparticles were synthesised by slow (dropwise) addition of 10 mL of 0.32 mM chloroauric acid solution into 15 mL of diluted gold colloid formed in experiment 'I'. Diameter = 9.1 ± 0.7 nm (Reprinted from [26] under CCA terms)

joshi@iitk.ac.in

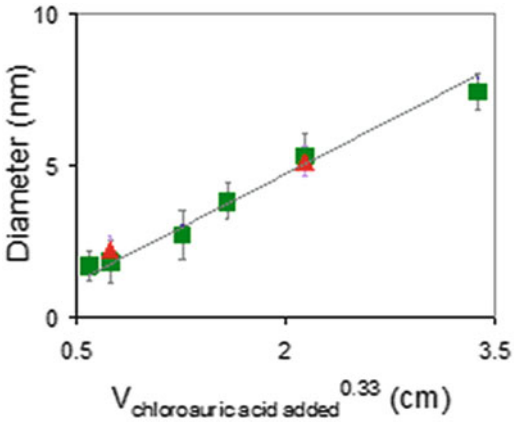

Fig. 10 A plot of expected and observed nanoparticle diameter as a function of the amount of the 1/3 power of the moles (equivalent to volume) of chloroauric acid added. The agreement between the predicted and observed diameters indicates that the slow (dropwise) addition process is akin to a one-shot nucleation-seeded growth process. *Triangle* and *square symbols* represent two different sets of experiment

is used. Thermal oxidation of citrate solution by dissolved oxygen can result in formation of acetone dicarboxylic acid and lead to faster reaction. To investigate this possibility, an experiment was performed by adding boiling citrate solution into boiling chloroauric acid. Figure 12c shows the digital images of the reaction mixture during the synthesis. The time taken for the formation of gold nanoparticles was similar to classical citrate method and it resulted in nanoparticles of size 14.0 ± 2.2 nm indicating that boiling of citrate solution does not significantly affect the synthesis.

Further experiments were performed by adding concentrated reactants into boiling water rather than diluting one of the reactant prior to reaction. Addition of citrate solution into boiling water followed by chloroauric acid resulted in faster reaction and smaller nanoparticles (8.1 ± 1.1 nm), while adding chloroauric acid into boiling water followed by citrate solution resulted in slower reaction and bigger nanoparticles (13.5 ± 2.3 nm). These experiments clearly prove that thermal degradation of citrate into acetone dicarboxylic acid, during the timescales involved in heating the reactants, does not account for the observed effects. To confirm the role of chloroauric acid reactivity, two further experiments were carried out: (1) the pH of the chloroauric acid solution was adjusted to be 3.2, similar to the classical citrate method, prior to addition into citrate, and (2) the pH of chloroauric acid solution was adjusted to 1.6 and citrate was added into it. Figure 12d–e shows that the kinetics is only affected by the initial pH of chloroauric acid solution and not by the mode of addition. However, the stability of the colloidal solution is enhanced when adding chloroauric acid at pH 1.6 into citrate solution.

Remarkably, the order of addition has a significant effect even when the observed induction periods were of the order of 100 s. An autocatalytic step in the oxidation of citrate by chloroauric acid is speculated to be responsible for this 'memory' effect, i.e. the presence of reactive chloroauric acid for short duration (5 s) during initial blending is sufficient to yield some acetone dicarboxylic acid, which then sustains the reaction.

joshi@iitk.ac.in

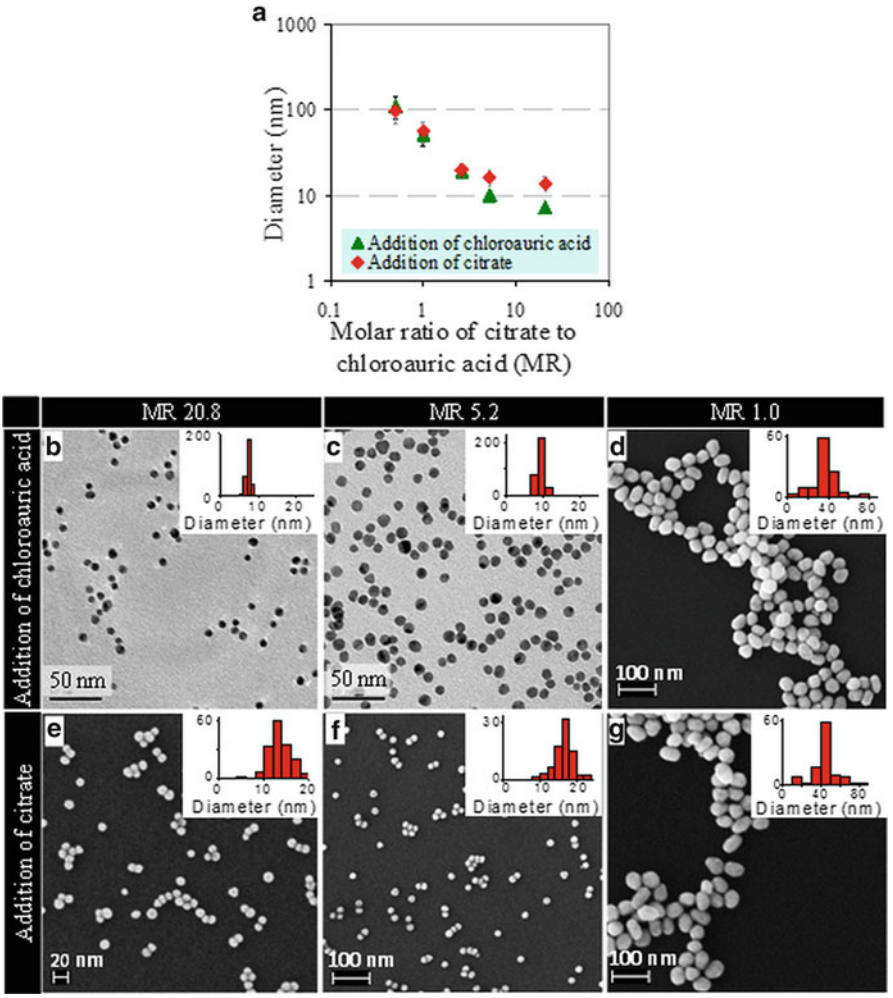

Fig. 11 Effect of reversing the order of addition of reactants. (**a**) Plot showing the variation of the mean particle size with the molar ratio for the two different modes of addition. The error bars represent one standard deviation. $HAuCl_4$ concentration was maintained constant at 25.4 mM. (**b**–**g**) Representative images with particle size histograms as *insets* are shown for colloids synthesised at three different molar ratios (MR) by the two different modes of addition of reactants. (**b**) MR = 20.8, gold chloride into citrate, diameter = 7.2 ± 0.8 nm. (**c**) MR = 5.2, gold chloride into citrate, diameter = 10.0 ± 1.0 nm. (**d**) MR = 1, gold chloride into citrate, diameter = 52.0 ± 15 nm. (**e**) MR = 20.8, citrate into gold chloride, diameter = 13.6 ± 2.7 nm. (**f**) MR = 5.2, citrate into gold chloride, diameter = 16.1 ± 3.3 nm. (**g**) MR = 1, citrate into gold chloride, diameter = 56.0 ± 15 nm (Reprinted from [27] with permission from Elsevier)

joshi@iitk.ac.in

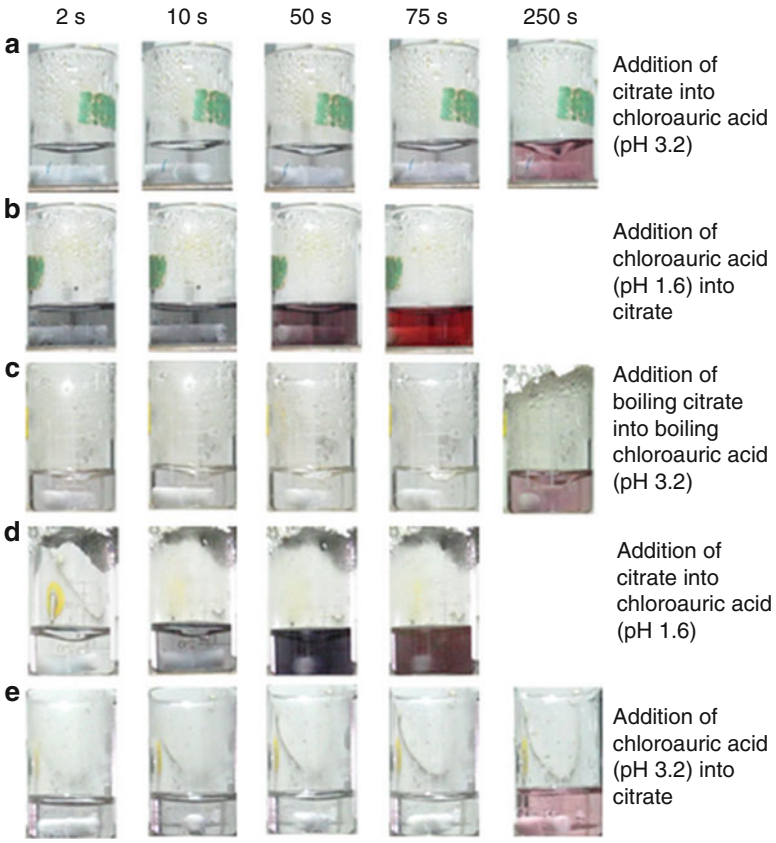

Fig. 12 Digital images of the reaction mixture taken during the course of nanoparticle synthesis. The MR value was 20.8 in all the above experiments. (**a**) Addition of citrate into boiling chloroauric acid (pH 3.2), standard Turkevich method. (**b**) Addition of chloroauric acid (pH 1.6) into boiling citrate. (**c**) Addition of citrate solution boiled for 10 min prior to addition into chloroauric acid (pH 3.2). (**d**) Addition of citrate into boiling chloroauric acid (pH 1.6). (**e**) Addition of chloroauric acid (pH 3.2) into boiling citrate (Color figure online) (Reprinted from [27] with permission from Elsevier)

5 Continuous-Flow Synthesis of Metal Nanoparticles

A primary objective of our project was to synthesise sub-10 nm metal nanoparticles in a continuous fashion using aqueous-phase processes. To achieve this, a simple coaxial flow microreactor setup was fabricated by moulding polydimethylsiloxane (PDMS) as shown in Fig. 13a. The metal salt was pumped through the inner tube, while tannic acid flowed around the core to avoid undesirable deposition and growth caused by adsorption of metal salt solutions on the reactor walls. The initial pH of the reagents was adjusted to ensure rapid reduction of metal salt by

joshi@iitk.ac.in

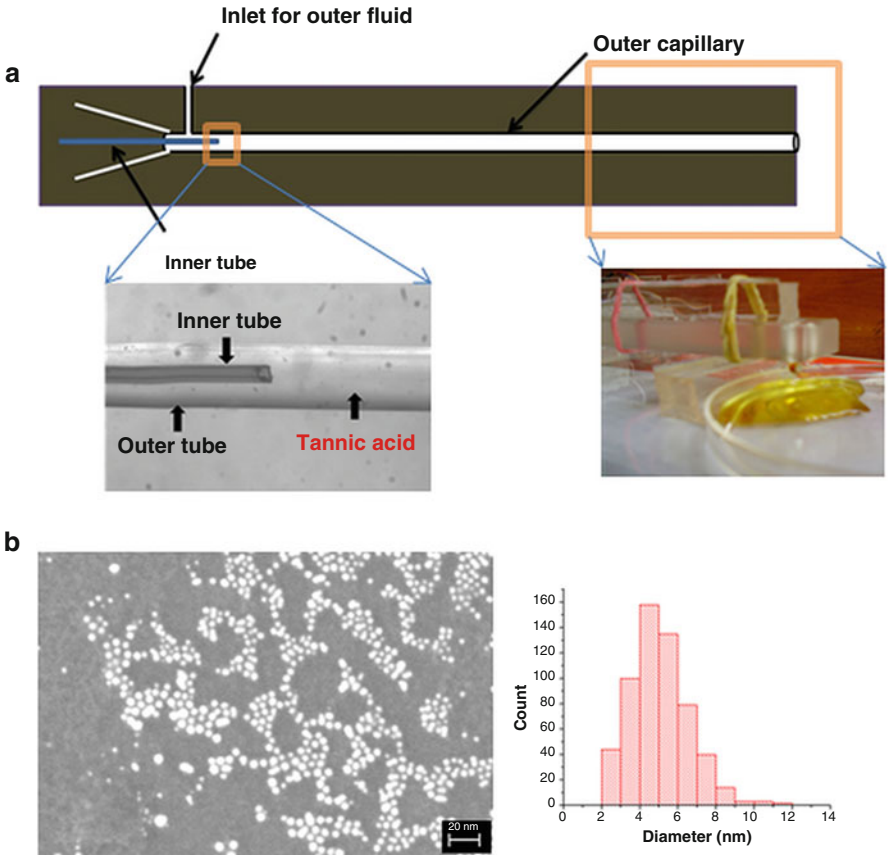

Fig. 13 (**a**) Schematic of the coaxial flow PDMS-based microchannel reactor along with digital images of the corresponding *insets*. The *yellow* colour of the collected solution reflects the formation of silver nanoparticles in this case. The inner diameter of the flow channel is 1 mm and it has a 150 μm capillary inserted coaxially at the entrance. Metal salt is introduced through the inner capillary, while tannic acid flows outside. (**b**) Representative SEM image of gold nanoparticles synthesised using the coaxial flow microchannel reactor and a histogram representing the corresponding size distribution (Color figure online)

tannic acid molecules. Complete conversion of the metal salt into silver or gold nanoparticles was found to occur for residence times of the order of 10 s, under the conditions of high reactivity in tune with earlier kinetic measurements. Interestingly, the nanoparticle size distribution was found to be similar to batch experiments at steady-state conditions (Fig. 13b) and was found to be insensitive to variations in flow velocities.

Microchannel flows can provide uniform and repeatable heat and mass transport conditions, which is purported to help in enhancing the reproducibility of nanoparticle synthesis; however, the widespread use and 'numbering-up' of microchannels

joshi@iitk.ac.in

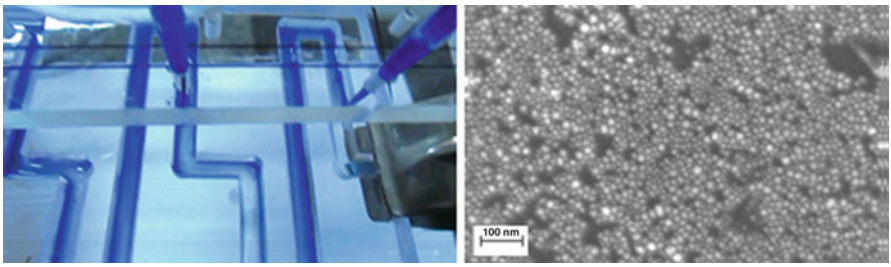

Fig. 14 Photograph of a novel flow reactor for metal nanoparticle synthesis. The channels were formed by cutting 2 mm wide × 2 mm deep slots into a PMMA sheet. The *blue colour* is due to the dye used for visualisation of the flow pattern in the reactor. During nanoparticle synthesis, tannic acid flows through the channels, while metal salt is added dropwise at selected points using syringes. A representative FESEM image of gold nanoparticles synthesised using the reactor is shown. The throughput in terms of gold was 1 g/h, and the average size of the gold nanoparticles was ∼10 nm (Color figure online)

are hindered by large pressure drops due to small channel sizes, leading to very high power requirements for pumping the reagents. As our earlier results suggested that speed of mixing and flow conditions had very little effect on the nanoparticle size distribution, as long as their reactivity was tuned by choosing appropriate feed conditions, we designed a simple gravity-fed open channel reactor with multiple feed inlets to mimic the dropwise addition protocol for synthesising monodisperse gold nanoparticles (Fig. 14). Salient features of our process design are the very high throughput (g/h) vis-à-vis typical throughput values of microchannel reactors (mg/h) and the negligible power requirements for pumping liquids. The particle size distribution was found to be consistent with earlier batch experiments at steady-state conditions.

6 Reactive Inkjet Deposition of Metal Nanoparticles

Paper-based electronics is an emerging field with applications focused on low-cost electronic circuits for human as well as structural diagnostics, ubiquitous sensor networks, etc. A key process in the formation of such circuits is the fabrication of patterned, conductive features on paper, preferably using low-cost roll-to-roll compatible processes. In this context, inkjet printing is one of the foremost contenders for fabricating patterned features on paper. Metal nanoparticle or carbon-based inks are typically used to fabricate patterned conductive features on paper using inkjet printing tools. However, the complex rheology and very high particulate content required to form conductive features require the use of sophisticated inkjet deposition tools, which hinder their adaptation for low-cost device fabrication.

The core-flow geometry for microchannel reactors was adapted after preliminary experiments in a Y-channel micromixer led to undesirable deposition on reactor

joshi@iitk.ac.in

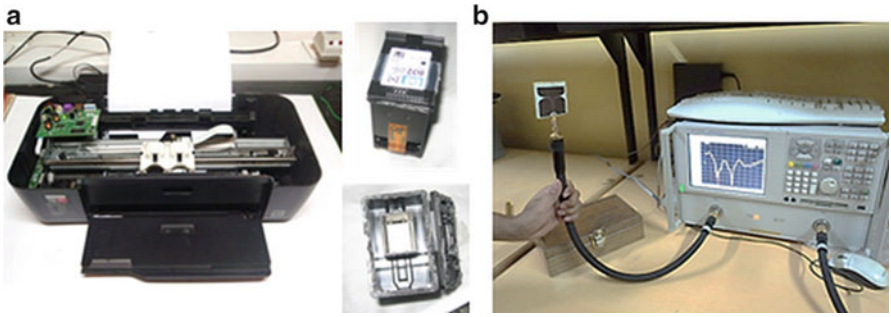

Fig. 15 (**a**) Photograph of the HP Deskjet 1000 printer used along with cartridges used for reactive inkjet printing. (**b**) Digital photographs of performance characterisation of UWB antenna fabricated on paper by using reactive inkjet printing and electroless deposition. The electrical performance of such paper-based antennas was found to be equivalent to that of antennas having the same design but fabricated using lithographic techniques on conventional RF substrates

walls by reduction of adsorbed metal salts. Such deposits were seen to form within seconds and also grow with extended exposure to the reagents. Although undesirable during bulk synthesis, the sturdy deposits formed rapidly, suggesting a simple route to fabricate conductive features on paper using office inkjet printers. We used an HP Deskjet 1000 printer and used reagent-filled ink cartridges to deposit silver nitrate and alkaline tannic acid solution sequentially on paper; desired patterns were generated using a standard computer interface. Silver nanoparticles formed *in situ* on the printed portions of the paper within seconds. This process represents a high-throughput method for synthesis and incorporation of metal nanoparticles into functional products. These silver nanoparticle patterns were further used as catalysts to generate conductive copper features on paper, using electroless plating. As a proof of concept, an ultrawideband (UWB) antenna was fabricated based on design from the literature (Fig. 15). The performance of the paper-based antenna was found to be equivalent to that reported for a similar antenna fabricated using conventional lithographic techniques [29].

7 Summary

A rapid, green, room temperature process for the synthesis of 2–20 nm gold and silver nanoparticles was developed. By simply altering the pH of the reagent solutions and modifying the mode of addition of reagents, monodisperse gold and silver nanoparticles were synthesised using tannic acid as the reducing and stabilising agent. An organiser-facilitated nucleation model was found to be suitable for describing the kinetics of nanoparticle formation. Similarly, reversing the order of addition in the widely used citrate method was found to result in highly monodisperse sub-10 nm gold nanoparticles. These results represent a significant

joshi@iitk.ac.in

advance in our knowledge of metal nanoparticle formation, especially considering the fact that these recipes have been widely studied for more than 100 years. Building upon this knowledge, high-throughput continuous-flow processes for the synthesis of gold and silver nanoparticles have been developed. Our results show that sub-10 nm gold and silver nanoparticles can be produced in continuous-flow reactors operated at room temperature. Furthermore, a low-cost process for the fabrication of conductive patterns on paper using an office inkjet printer was demonstrated. This process will be very useful for producing low-cost RFID tags and biodiagnostic devices on paper. Further investigations are required to understand the influence of flow patterns on nanoparticle size distribution for the continuous-flow reactor developed in this project.

Acknowledgements We gratefully acknowledge support from IRHPA scheme of DST. We also acknowledge the inputs of our students, project assistants and collaborators over the last 6 years. Excerpts have been reprinted with permission from Elsevier and Indian Academy of Sciences.

References

1. Pitkethly MJ (2004) Nanomaterials–the driving force. Mater Today 7:20–29
2. Ghosh P, Han G, De M, Kim CK, Rotello VM (2008) Gold nanoparticles in delivery applications. Adv Drug Deliv Rev 60:1307–1315
3. Muralidharan G, Bhat N, Santhanam V (2011) Scalable processes for fabricating non-volatile memory devices using self-assembled 2D arrays of gold nanoparticles as charge storage nodes. Nanoscale 3:4575–4579
4. Brown C, Bushell G, Whitehouse M, Agrawal DS, Tupe SG, Paknikar KM, Tiekink E (2007) Nanogoldpharmaceutics. Gold Bull 40:245–250
5. Wilson R (2008) The use of gold nanoparticles in diagnostics and detection. Chem Soc Rev 37:2028–2045
6. Santhanam V, Andres RP (2009) Metal nanoparticles: self-assembly into electronic nanostructures. In: Contescu CI, Putyera K (eds) Dekker encyclopedia of nanoscience and nanotechnology, 2nd edn. CRC Press, Boca Raton, pp 2079–2090
7. Feldheim DL, Colby AF Jr (2001) Metal nanoparticles: synthesis, characterization, and applications. CRC Press, New York
8. Thompson D (2007) Michael Faraday's recognition of ruby gold: the birth of modern nanotechnology. Gold Bull 40:267–269
9. Weiser HB (1933) Inorganic colloid chemistry. Wiley, New York
10. Slot JW, Geuze HJ (1985) A new method of preparing gold probes for multiple-labeling cytochemistry. Eur J Cell Biol 38:87–93
11. Frens G (1973) Controlled nucleation for the regulation of the particle size in monodisperse gold suspensions. Nat Phys Sci 241:20–22
12. Turkevich J (1951) A study of the nucleation and growth processes in the synthesis of colloidal gold. Discuss Faraday Soc 11:55–75
13. Perala SRK, Kumar S (2013) On the mechanism of nanoparticle synthesis in Brust-Schiffrin method. Langmuir 29:9863–9873
14. Hutchison JE (2008) Greener nanoscience: a proactive approach to advancing applications and reducing implications of nanotechnology. ACS Nano 2:395–402
15. Dykman LA, Bogatyrev VA (2007) Gold nanoparticles: preparation, functionalisation and applications in biochemistry and immunochemistry. Russ Chem Rev 76:181–194

joshi@iitk.ac.in

16. Ostwald CWW (1917) An introduction to theoretical and applied colloid chemistry. Wiley, New York
17. Mühlpfordt H (1982) The preparation of colloidal gold particles using tannic acid as an additional reducing agent. Experientia 38:1127–1128
18. Bulut E, Özacar M (2009) Rapid, facile synthesis of silver nanostructure using hydrolyzable tannin. Ind Eng Chem Res 48:5686–5690
19. Tian X, Wang W, Cao G (2007) A facile aqueous-phase route for the synthesis of silver nanoplates. Mater Lett 61:130–133
20. Sivaraman SK, Elango I, Kumar S, Santhanam V (2009) A green protocol for room temperature synthesis of silver nanoparticles in seconds. Curr Sci India 97:1055–1059
21. Cruz BH, Díaz-Cruz JM, Ariño C, Esteban M (2000) Heavy metal binding by tannic acid: a voltammetric study. Electroanalysis 12:1130–1137
22. Bors W, Foo LY, Hertkorn N, Michel C, Stettmaier K (2001) Chemical studies of proanthocyanidins and hydrolyzable tannins. Antioxid Redox Signal 3:995–1008
23. Martinez-Castanon G, Nino-Martinez N, Martinez-Gutierrez F, Martinez-Mendoza J, Ruiz F (2008) Synthesis and antibacterial activity of silver nanoparticles with different sizes. J Nanopart Res 10:1343–1348
24. Liu J, Qin G, Raveendran P, Ikushima Y (2006) Facile "green" synthesis, characterization, and catalytic function of β-D-glucose-stabilized au nanocrystals. Chem Eur J 12:2131–2138
25. Belloni J (2006) Nucleation, growth and properties of nanoclusters studied by radiation chemistry: application to catalysis. Catal Today 113:141–156
26. Sivaraman SK, Kumar S, Santhanam V (2010) A room temperature synthesis of gold nanoparticles: size control by slow addition. Gold Bull 43:275–286
27. Sivaraman SK, Kumar S, Santhanam V (2011) Monodisperse sub-10 nm gold nanoparticles by reversing the order of addition in Turkevich method – the role of chloroauric acid. J Colloid Interface Sci 361:543–547
28. Kumar S, Gandhi KS, Kumar R (2007) Modeling of formation of gold nanoparticles by citrate method. Ind Eng Chem Res 46:3128–3136
29. Kumar S, Bhat V, Vinoy KJ, Santhanam V (2013) Using an office inkjet printer to define the formation of copper films on paper. IEEE Trans Nanotechnol 13:160–164

joshi@iitk.ac.in